[14] Hansen, C. F., "Approximations for the thermodynamic and transport properties of high-temperature air," NASA TR R-50 (1959).

[15] Gaydon, A. G. and Hurle, I. R., "Measurement of times of vibrational relaxation and dissociation behind shock waves in N_2, O_2, air, CO, CO_2 and H_2," *Eighth Symposium on Combustion, 1960* (The Combustion Institute, Baltimore, Md., 1962), pp. 309–318.

[16] Brabbs, T. A., Belles, F. E., and Zlatarich, S. A., "Shock-tube study of carbon dioxide dissociation rate," J. Chem. Phys. **38,** 1939–1944 (1963).

[17] Davies, W. O., "Radiative energy transfer on entry into Mars and Venus," IIT Research Institute Rept. IITRI-T200-6 (October 1963); also "Carbon dissociation at 3500° to 6000°K," J. Chem. Phys. **41,** 1846–1852 (1964).

[18] Gray, D. E. (ed.), *American Institute of Physics Handbook* (McGraw-Hill Book Co., Inc., New York, 1963), 2nd ed., pp. 4-315–4-330.

[19] Plass, G. N., "Models for spectral band absorption," J. Opt. Soc. Am. **48,** 690–703 (1958).

[20] Plass, G. N., "Useful representations for measurements of spectral band absorption," J. Opt. Soc. Am. **50,** 868–875 (1960).

[21] Malkmus, W., "Infrared emissivity of carbon dioxide (4.3-μ band)," J. Opt. Soc. Am. **53,** 951–961 (1963); also General Dynamics/Astronautics Rept. AE62-0204 (February 1962).

[22] Ferriso, C. C., "High-temperature spectral absorption of the 4.3-micron CO_2 band," J. Chem. Phys. **37,** 1955–1961 (1962).

[23] Steinberg, M. and Davies, W. O., "High-temperature absorption of carbon dioxide at 4.40 μ," J. Chem. Phys. **34,** 1373–1377 (1961).

[24] Oppenheim, U. P. and Ben-Aryeh, Y., "Statistical model applied to the region of the ν_3 fundamental of CO_2 at 1200°K," J. Opt. Soc. Am. **53,** 344–350 (1963).

[25] Sulzmann, K. G. P., "High temperature shock tube CO_2–transmission measurements at 4.25μ," J. Quant. Spectry. Radiative Transfer **4,** 375–413 (1964).

[26] Herzfeld, K. F. and Litovitz, T. A., *Absorption and Dispersion of Ultrasonic Waves* (Academic Press Inc., New York, 1959), pp. 246–250.

[27] Smiley, E. F. and Winkler, E. H., "Shock-tube measurements of vibrational relaxation," J. Chem. Phys. **22,** 2018–2022 (1954).

[28] Griffith, W., Brickl, D., and Blackman, V., "Structure of shock waves in polyatomic gases," Phys. Rev. **102,** 1209–1216 (1956).

[29] Daen, J. and de Boer, P. C. T., "Some studies on argon, helium, and carbon dioxide with an integrated-schlieren instrumented shock tube," J. Chem. Phys. **36,** 1222–1228 (1962).

[30] Johannesen, N. H., Zienkiewicz, H. K., Blythe, P. A., and Gerrard, J. H., "Experimental and theoretical analysis of vibrational relaxation regions in carbon dioxide," J. Fluid Mech. **13,** 213–224 (1962); also Zienkiewicz, H. K., Johannesen, N. H., and Gerrard, J. H., "Further results on the over-all density ratios of shock waves in carbon dioxide," J. Fluid Mech. **17,** 267–270 (1963).

[31] Witteman, W. J., "Vibrational relaxation in carbon dioxide. II," J. Chem. Phys. **37,** 655–661 (1962).

[32] Slobodskaia, P. V., Izv. Akad. Nauk SSSR, Ser. Fiz. **12,** 656 (1948); quoted in Ref. 26.

[33] Slobodskaia, P. V. and Gasilevich, E. S., "Development of a method of determining the relaxation time of the vibratory state of molecules using a spectrophone," Opt. Spectry. (USSR) (English transl.) **7,** 58–62 (1959).

[34] Jacox, M. E. and Bauer, S. H., "Collisional energy exchange in gases. Use of the Spectrophone for studying relaxation processes in carbon dioxide," J. Phys. Chem. **61,** 833–844 (1957).

[35] Camac, M., "CO_2 relaxation processes in shock waves," Avco-Everett Research Lab. Research Rept. 194 (October 1964).

APRIL 1965 AIAA JOURNAL VOL. 3, NO. 4

Unsteady Three-Dimensional Laminar Jet Mixing of a Compressible Fluid

S. I. Pai*
University of Maryland, College Park, Md.

The fundamental equations of an unsteady three-dimensional laminar jet mixing of a compressible fluid have been discussed. These equations are simplified by introducing two stream functions. Finally, the unsteady jet flow that deviates slightly from an unsteady uniform flow is studied in detail. It was found that, for arbitrary three-dimensional jets, the velocity and temperature distributions tend to be axisymmetrical at large time-from-start and far downstream. Some numerical examples are given.

I. Introduction

MOST of the free jet-mixing problems consider the cases of steady flow[2] of two-dimensional or axisymmetrical or rotationally symmetrical[3–5] configuration in which the flow variables are functions of two spatial variables only. Little has been done for the case of general three-dimensional flow in which the flow variables are functions of all three spatial variables as well as time. In practice, the jet flow may oscillate, and the general stream in which the jet flow is located may be unsteady itself. Furthermore, the directions of the general stream and of the jet may not be the same. Hence, the three-dimensional character of the jet-mixing problem is important. In this paper, we discuss the general behavior of an unsteady three-dimensional jet-mixing region in a uniform stream of a viscous and compressible ideal gas.

We consider a jet issuing from a nozzle into an unsteady freestream. The deviation of the direction of the jet from that of the freestream is assumed to be small. We further assume that the deviation of the cross section of the exit of the nozzle from a circular cross section is also small. As a result, the radial component of the jet flow will be small, and the jet behaves as a free boundary-layer flow with a large gradient in the radial (r) direction. If we take x as the direc-

Received June 4, 1964; revision received December 31, 1964. This research was supported in part by the U.S. Air Force through the Air Force Office of Scientific Research under Grant No. AFOSR 141-65. The numerical computations were carried out in the Computer Sciences Center, University of Maryland by H. H. Chu.

* Research Professor, Institute for Fluid Dynamics and Applied Mathematics. Associate Fellow Member AIAA.

tion of the jet, it is convenient to use the three-dimensional boundary-layer equations in cylindrical coordinates (r, x, θ) where θ is the angular coordinate.

We assume that the freestream deviates slightly from a rotationally symmetrical flow so that the inviscid flow outside the jet-mixing region may be written as

$$\begin{aligned} u_\infty &= u_{\infty 0}(x, t) + \epsilon f_1(x, \theta, t) \\ w_\infty &= w_{\infty 0}(x, t) + \epsilon f_2(x, \theta, t) \\ p_\infty &= p_{\infty 0}(x, t) = \epsilon f_3(x, \theta, t) \\ \rho_\infty &= \rho_{\infty 0}(x, t) + \epsilon f_4(x, \theta, t) \\ H_\infty &= H_{\infty 0}(x, t) + \epsilon f_5(x, \theta, t) \end{aligned} \tag{1}$$

where u and w are, respectively, the axial $(x-)$ and tangential $(\theta-)$ velocity components of the flow; p, ρ, and H are the pressure, density, and enthalpy of the fluid, respectively; the subscript ∞ refers to the value at the edge of the jet-mixing region and subscript 0 refers to the corresponding value for a rotationally symmetrical case. Thus, the velocity $w_{\infty 0}$ is the swirling velocity of the freestream. The parameter ϵ is a small quantity that characterizes the deviation from the rotationally symmetrical flow. The functions f_1 to f_5 are known functions of x, θ, and t in our problem, where t is the time.

II. Fundamental Equations

We use a cylindrical coordinate system fixed with respect to the nozzle from which the jet flow issues. The nozzle moves with an axial velocity $U(t)$, which is in general a known function of time and may be a constant. Our fundamental equations in this coordinate system are as follows:

Equation of Continuity

$$\frac{\partial \rho r}{\partial t} + \frac{\partial \rho r u}{\partial x} + \frac{\partial \rho w}{\partial \theta} + \frac{\partial \rho r v}{\partial r} = 0 \tag{2}$$

where v is the radial velocity component.

Equations of Motion

$$\rho \frac{\partial u}{\partial t} + \rho u \frac{\partial u}{\partial x} + \rho \frac{w}{r} \frac{\partial u}{\partial \theta} + \rho v \frac{\partial u}{\partial r} = - \frac{\partial p}{\partial x} + \rho \frac{dU}{dt} + \frac{1}{r} \frac{\partial}{\partial r} \left(\mu r \frac{\partial u}{\partial r} \right) \tag{3}$$

$$\rho \frac{\partial w}{\partial t} + \rho u \frac{\partial w}{\partial x} + \rho \frac{w}{r} \frac{\partial w}{\partial \theta} + \rho \frac{v}{r} \frac{\partial w r}{\partial r} = - \frac{1}{r} \frac{\partial p}{\partial \theta} + \frac{1}{r^2} \frac{\partial}{\partial r} \left[\mu r \left(\frac{\partial w}{\partial r} - \frac{w}{r} \right) \right] \tag{4}$$

$$\rho w^2 / r = \partial p / \partial r \tag{5}$$

Energy Equation

$$\rho \frac{\partial H_s}{\partial t} + \rho u \frac{\partial H_s}{\partial x} + \rho \frac{w}{r} \frac{\partial H_s}{\partial \theta} + \rho v \frac{\partial H_s}{\partial r} = \rho u \frac{dU}{dt} + \frac{\partial p}{\partial t} + \frac{1}{r} \frac{\partial}{\partial r} \left(\frac{\mu r}{P_r} \frac{\partial H_s}{\partial r} \right) + \frac{1}{r} \frac{\partial}{\partial r} \left[\mu r \left(1 - \frac{1}{P_r} \right) \left(u \frac{\partial u}{\partial r} + w \frac{\partial w}{\partial r} \right) - \mu w^2 \right] \tag{6}$$

where $H_s = H + \frac{1}{2}(u^2 + w^2)$ is the stagnation enthalpy; μ is the coefficient of viscosity; and $P_r = \kappa / \mu C_P$ is the Prandtl number. We shall assume that C_P is constant in our analysis.

The boundary-layer approximations have been used in Eqs. (3–6). It is assumed that $\partial(\ )/r\partial\theta$ is of the same order of magnitude as $\partial(\ )/\partial x$ and both are smaller than $\partial(\ )/\partial r$.

Equation of State

$$p = \rho R_0 T \tag{7}$$

where R_0 is the gas constant.

III. Some Transformations of the Fundamental Equations

The fundamental equations of Sec. II may be simplified by introducing two stream functions ψ and ϕ such that

$$\rho u r = \frac{\partial \psi}{\partial r} \qquad \rho w = \frac{\partial \phi}{\partial r}$$
$$\rho r v = - \frac{\partial \psi}{\partial x} - \frac{\partial \phi}{\partial \theta} - \frac{\partial}{\partial t} \int_0^r \rho r dr \tag{8}$$

When the flow is rotationally symmetrical, the stream function ψ reduces to the ordinary stream function for axisymmetrical flow. Substituting Eq. (8) into Eq. (2), the equation of continuity (2) is automatically satisfied. Hence, if we use the stream functions ψ and ϕ instead of velocity components u, v, and w, we need not consider the equation of continuity.

For the case of a compressible fluid, it is convenient to use the variables R, X, τ, and Θ instead of r, x, t, and θ such that

$$R = \int_0^r \rho r dr \qquad X = x \qquad \tau = t \qquad \Theta = \theta \tag{9}$$

Then we have

$$u = \psi_R \qquad w = r \phi_R$$
$$v = - \frac{1}{\rho r} \left(\psi_X + \frac{\partial R}{\partial x} \psi_R + \frac{\partial R}{\partial t} + \phi_\Theta + \frac{\partial R}{\partial \theta} \phi_R \right) \tag{10}$$

where subscripts R, X, τ, and Θ refer to the partial differentiations.

Substituting Eqs. (9) and (10) into Eqs. (3–6), we have

$$\psi_{R\tau} + \psi_R \psi_{RX} + \phi_R \psi_{R\Theta} - (\psi_X + \phi_\Theta) \psi_{RR} = - \frac{1}{\rho} p_X - \frac{1}{\rho} \frac{\partial R}{\partial X} p_R + \frac{dU}{dt} + (\mu \rho r^2 \psi_{RR})_R \tag{11}$$

$$\phi_{R\tau} + \psi_R \phi_{RX} + \phi_R \phi_{R\Theta} - (\psi_X + \phi_\Theta) \phi_{RR} - \frac{1}{\rho r^2} (\psi_X + \phi_\Theta) \phi_R - \left(\psi_X + \frac{\partial R}{\partial x} \psi_R + \frac{\partial R}{\partial t} + \phi_\Theta + \frac{\partial R}{\partial \theta} \phi_R \right) \frac{\phi_R}{\rho r^2} = - \frac{1}{\rho r^2} \left(p_\Theta + \frac{\partial R}{\partial \theta} p_R \right) + \frac{1}{r^2} \times (\mu \rho r^4 \phi_{RR})_R \tag{12}$$

$$p_R = \phi_R^2 \tag{13}$$

$$H_{S\tau} + \psi_R H_{SX} + \phi_R H_{S\Theta} - (\psi_X + \phi_\Theta) H_{SR} = \psi_R \frac{dU}{dt} + \frac{1}{\rho} \left(p + \frac{\partial R}{\partial t} p_R \right) + \left(\frac{\mu \rho r^2}{P_r} H_{SR} \right)_R + \left[\rho \mu r^2 \left(1 - \frac{1}{P_r} \right) \{ \psi_R \psi_{RR} + r \phi_R (r \phi_R)_R \} - \mu r^2 \phi_R^2 \right]_R \tag{14}$$

where r^2 is considered as a function of R, X, τ, and Θ from Eq. (9). Equations (11–14), together with Eq. (7), are the fundamental equations of unsteady three-dimensional free-mixing problems.

IV. Unsteady Jet Flow Deviates Slightly from an Unsteady Freestream

In order to show some essential features of unsteadiness and three dimensionality, we consider the case that there is a known unsteady freestream with axial velocity $U(\tau)$ only and that the resultant jet flow deviates slightly from this mean flow of axial velocity $U(\tau)$. The deviation may occur, for instance, because of small oscillation of the jet, or a small swirl, or a nonuniform initial velocity distribution along the tangential direction of the exit of the nozzle, or a combination of several of these causes. Under this condition, we may ex-

pand the variables of our problem in powers of a small parameter ϵ, which characterizes the deviation as follows:

$$Q = Q_0(\tau) + \epsilon Q_1(R, X, \tau, \Theta) + 0(\epsilon^2) \tag{15}$$

where Q may be ψ, p, ρ, ϕ, or H_S and $\psi_0 = RU(\tau)$, p_0 and ρ_0, and H_0 are constants and $H_{S0} = H_0 + \frac{1}{2}U^2(\tau)$.

From Eqs. (9) and (15) we have

$$r^2 = (2/\rho_0)R + \epsilon r_1^2(R, X, \tau, \Theta) + 0(\epsilon^2) \tag{16}$$

Substituting Eqs. (15) and (16) into Eqs. (11–14) and neglecting terms of order of ϵ^2 or higher, we have the equations for the first-order variables Q_1 as follows:

$$\psi_{1R\tau} + U\psi_{1RX} = -(1/\rho_0)p_{1X} + 2\mu_0(R\psi_{1RR})_R \tag{17a}$$

$$H_{S1\tau} + UH_{S1X} = \psi_{1R}U_\tau + \frac{1}{\rho_0}p_{1\tau} + \frac{2\mu_0}{P_r}(RH_{S1R})_R + \left[2R\mu_0\left(1 - \frac{1}{P_r}\right)U\psi_{1RR}\right]_R \tag{17b}$$

$$p_R = 0 \tag{17c}$$

$$\phi_{1R\tau} + U\phi_{1RX} = -\frac{1}{2R}p_{1\Theta} + \frac{2\mu_0}{R}(R^2\phi_{1RR})_R \tag{17d}$$

Equations (17a–17c) are independent of angular coordinate Θ and linear. They are in exactly the same form as those of axisymmetrical flow. If the initial values of flow variables ψ_1 and H_{S1} are functions of Θ, it is evident that the variations of these variables with respect to Θ will remain unchanged downstream in the following manner:

If we develop the initial values in Fourier series of angular coordinate Θ, e.g.,

$$\psi_{1R}(R, 0, 0, \Theta) = \sum_{n=0}^{\infty}[A_n(R)\sin n\Theta + B_n(R)\cos n\Theta] \tag{18}$$

we may find the solution ψ_{1R} in the form

$$\psi_{1R}(R, X, \tau, \Theta) = \sum_{n=0}^{\infty}[\psi_{1RA_n}(R, X, \tau) \times \sin n\Theta + \psi_{1RB_n}(R, X, \tau)\cos n\Theta] \tag{19}$$

where ψ_{1RA_n} and ψ_{1RB_n} are, respectively, the solutions of axisymmetrical flow with initial values $A_n(R)$ and $B_n(R)$. In other words, the variations of ψ_{1R} and H_{S1R} in each plane, Θ = const, is the same as the corresponding axisymmetrical flow for first approximations. After the solutions in every plane of Θ are known, Eq. (19) gives the complete three-dimensional solution.† For first approximation, we only need to know how to obtain the solution of axisymmetrical flow in order to predicate the behavior of the general three-dimensional case.

V. The Solution of Axisymmetrical Flow

Now we are going to find the solution of an axisymmetrical flow in a nonsteady uniform stream $U(\tau)$. In this problem, we assume that the first-order pressure perturbation p_{1X} is zero because the outside flow is a uniform flow. Equations (17a) and (17b) may be written as

$$Q_\tau + UQ_X = 2\mu_0(RQ_R)_R \tag{20}$$

where Q may be either the perturbed x-wise velocity component ψ_{1R} or the perturbed enthalpy H_1.

If we make the transformation

$$t_1 = 2\mu_0\tau \qquad R = R \qquad X_1 = X - \int_0^\tau U(t)dt \tag{21}$$

† Because of the indeterminancy of Θ at $R = 0$, the solution does not hold at $R = 0$, but it gives the general trend at $R > 0$.

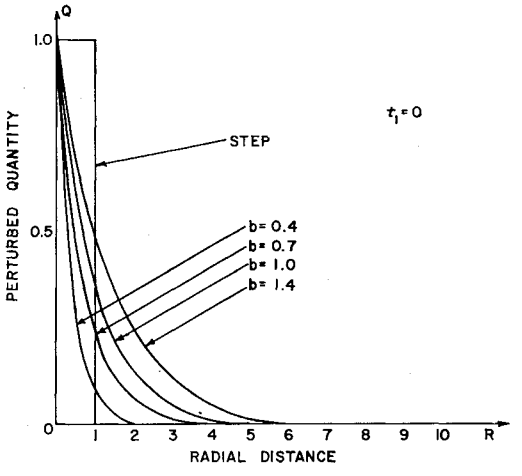

Fig. 1 Initial values of perturbed quantity.

Eq. (20) becomes

$$Q_{t_1} = (RQ_R)_R \tag{22}$$

The initial and boundary conditions for Q are

$$Q(R, 0) = g(R) \qquad Q(\infty, t_1) = 0 \tag{23}$$

The solution of Eq. (22) with conditions (23) is

$$Q(R, t_1) = \frac{1}{t_1}\exp\left(\frac{-R}{t_1}\right)\int_0^\infty \exp\left(-\frac{R'}{t_1}\right) \times I_0\left(\frac{2R^{1/2}R'^{1/2}}{t_1}\right)g(R')dR' \tag{24}$$

where I_0 is the modified Bessel function of zeroth order.

VI. Numerical Examples

Since, in terms of t_1 and R, the perturbed function Q does not depend on $U(\tau)$ explicitly, we may first find the universal solution Q from a given initial function $g(R)$ and then determine the flow field for various freestream velocity $U(\tau)$ from this universal solution Q. In order to bring out some general properties of the solution, we take a simple function for $g(R)$ as follows‡:

$$g(R) = A\exp(-R/b) \tag{25}$$

where A and b are arbitrary constants. Since it is well known that most of the velocity and temperature distributions in the jet-mixing region are close to exponential or error functions, Eq. (25) would give the essential features of the jet flow. Because Eq. (22) is linear, we may take $A = 1$ without loss of generality. We calculate Q from Eqs. (22) or (24) with $g(R)$ given by Eq. (25) with $b = 0.4$, 0.7, 1.0, and 1.4. We also calculate the case for $g(R)$ represented by a step function, i.e.,

$$g(R) = 1 \text{ for } 0 \leq R \leq 1 \qquad g(R) = 0 \text{ for } R \geq 1 \tag{26}$$

Equation (26) is one of the typical initial functions often used in jet-mixing analysis in which the boundary layer at the exit is negligible.

Figures 1–3 give some typical curves for $Q(R, t_1)$ for various initial functions at $t_1 = 0$, 1.0, and 5.0, respectively. Figure 4

‡ This distribution is equivalent to $g(r) = Ae^{-r^2/b}$, which has been used extensively in wake problems (see p. 10 of Ref. 1). Hence, the example should bring out the essential points of the present problem.

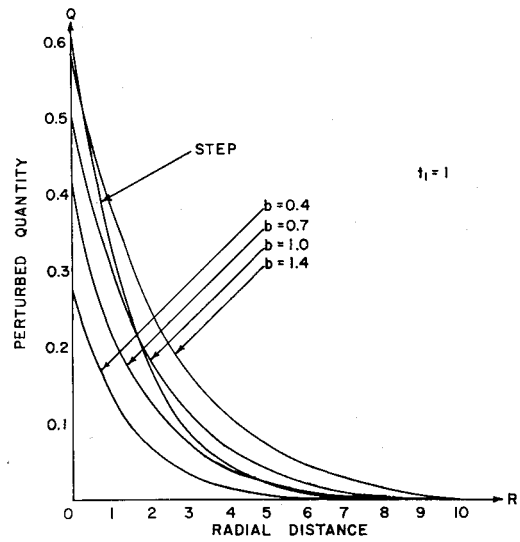

Fig. 2 Radiatial distribution of perturbed quantity at $t_1 = 1$.

shows the variations of the maximum values of Q with respect to t_1. It is seen that the larger the value of b, which characterizes the width of the initial jet, the slower the rate of decrease of Q_{max} will be. Since we have already normalized the initial velocity profiles (Fig. 1), the factor b represents the total "momentum" or "heat" excess in the jet flow. Thus the rate of decrease of Q_{max} decreases as the total "excess" of Q in the jet increases.

If we plot Q/Q_{max} vs R at various t_1, we have Figs. 5 and 6 for $t_1 = 1.0$ and $t_1 = 5.0$, respectively. The interesting result is that the profiles of Q/Q_{max} vs R tend to be similar for all of the initial functions at large value of t_1. In other words, at large t_1, e.g., $t_1 \geqq 5.0$, a single curve Q/Q_{max} vs R may be used to represent all initial functions (see Fig. 6). At small value of t_1, the variation Q/Q_{max} vs R depends greatly on the initial function (see Fig. 5).

The values of Q and Q_{max} given in Figs. 1–6 may be interpreted as the values of Q at a given point $X_1 = 0$, which may be arbitrarily chosen, e.g., at the exit of the nozzle at $t_1 = 0$; and at various values of t_1. Hence, the location $X_1 = 0$ is fixed in space. In order to obtain the value of Q at a location X fixed relative to the exit of the nozzle, we can find the value of X from t_1 by the transformation (21), i.e.,

$$X = \int_0^\tau U(t)dt \tag{27}$$

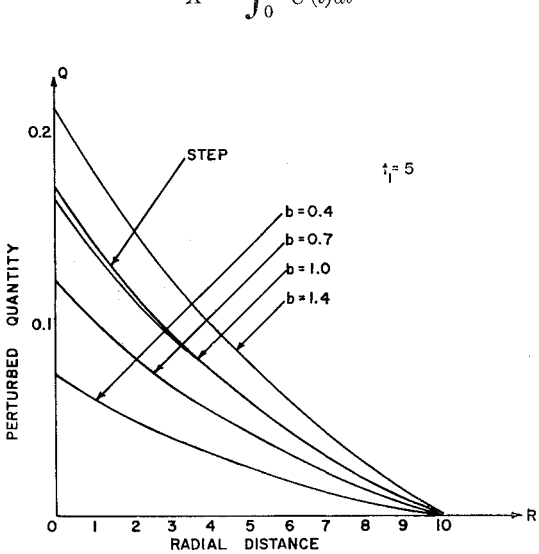

Fig. 3 Radiatial distribution of perturbed quantity at $t_1 = 5$.

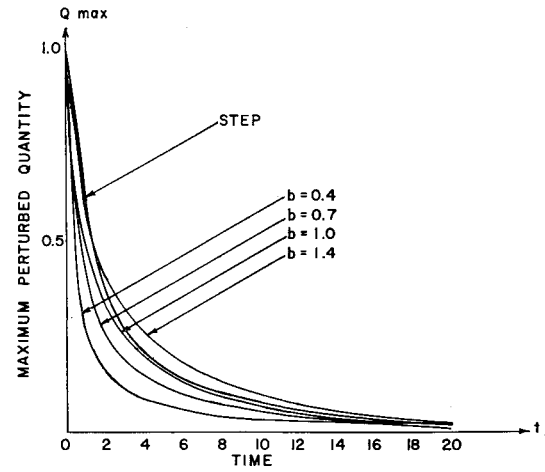

Fig. 4 Variations of maximum perturbed quantity with time.

Of course, the location X depends on the velocity of the nozzle $U(t)$. For steady-flow case, we have $U(t) = U = \text{const}$. Then Eq. (27) gives

$$x = Ut_1/2\mu_0 \quad \text{or} \quad t_1 = 2\mu_0 x/U \tag{28}$$

Equation (28) is the well-known transformation for the steady-flow case.

For an unsteady flow with velocity $U(\tau)$, since the initial value $g(R)$ corresponds to $X = 0$ and $\tau = 0$, the actual flow condition at $X = X$ and $\tau = 0$ corresponds to the value at $X = 0$ and $\tau = \tau_1$, where τ_1 is determined by Eq. (27) for a given value of X. From the value of τ_1, we have the corresponding value of $t_1 = 2\mu_0\tau_1$.

In Fig. 7, we plot X vs τ from Eq. (27) for the following cases:

$$U(\tau) = 1 + a\tau \tag{29}$$

(with $a = 0$, steady flow; $a = 0.1$, accelerated flow; and $a = -0.1$, decelerated flow; for the decelerated flow, the result for $\tau \geqq 10$ has no practical significance), and

$$U(\tau) = 1 + 0.5 \sin 0.2\tau \tag{30}$$

This represents an oscillating flow.

With the help of curves in Fig. 7, we can find the axial variation of Q_{max} at various time. Figure 8 shows some typical results at $\tau = 0$. For the oscillating flow (30), the curve lies between those of $a = 0$ and $a = 0.1$ because the

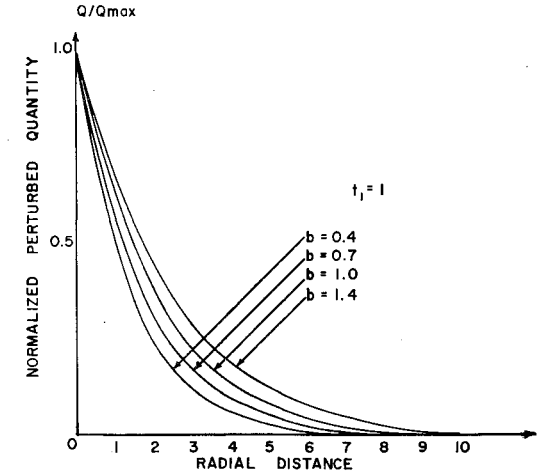

Fig. 5 Normalized radial distribution of perturbed quantity at $t_1 = 1$.

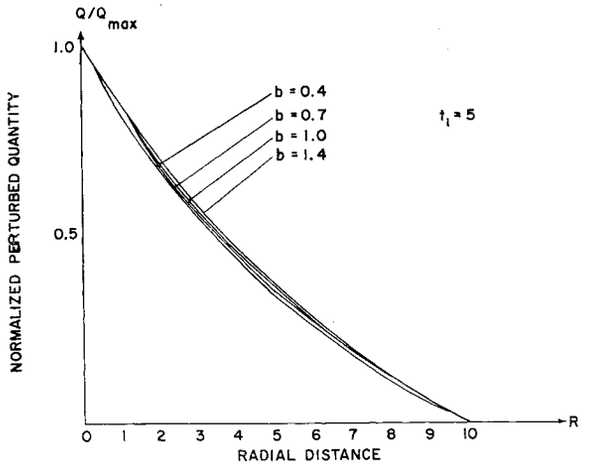

Fig. 6 Normalized radial distribution of perturbed quantity at $t_1 = 5$.

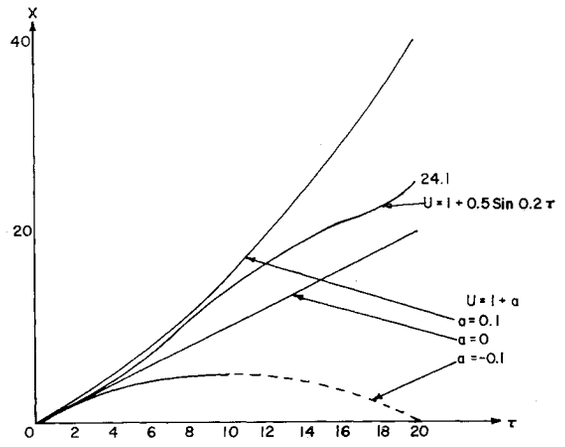

Fig. 7 $x - \tau$ diagram for various u (τ).

$x - \tau$ curve for this oscillating flow lies between those of $a =$ and $a = 0.1$.

VII. Conclusions

The following conclusions may be drawn from our analysis of three-dimensional unsteady laminar jet-mixing problems for a jet deviated slightly from an unsteady uniform flow:

1) The variations of axial velocity and enthalpy in each plane, $\Theta = \text{const}$, are the same as those of the corresponding axisymmetrical case.

2) If the initial profile $g(R)$ is the same, the perturbed quantity in the section with larger initial magnitude A will decrease faster than those with smaller A because the effective time t_1 to reduce the perturbed quantity to a fraction of its initial value is the same. As a result, the difference of the magnitudes of the perturbed quantity at various sections

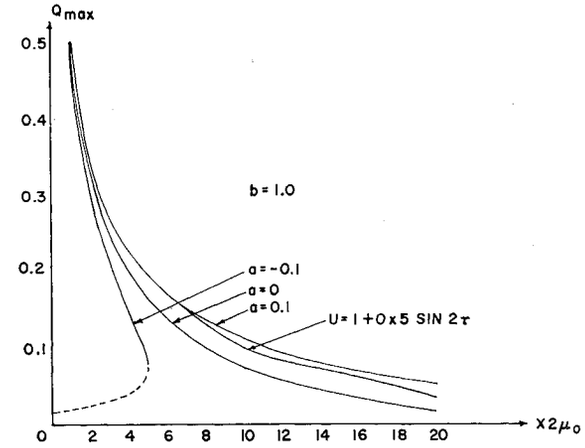

Fig. 8 Axial variation of Q_{max} at $= 0$.

Θ reduces downstream and the whole flow field of the jet-mixing region tends toward axisymmetrical distribution far downstream.[3]

3) For the same magnitude A but different initial profiles $g(R)$, the curve with broader initial distribution [large value of b in Eq. (25)] has a lower rate of decrease of Q_{max} with time t_1 (see Fig. 4).

4) The radial distributions of perturbed quantity (Fig. 6) tend to be similar for all initial functions for large values of t_1.

5) Combining conclusions 2 and 4, we may draw the final conclusion that, in general, the jet flow tends to be axisymmetrical far downstream because, first, all the profiles tend to be similar, and then, for similar profiles, the difference of magnitude decreases downstream. A similar result has been found by Steiger and Bloom for a special case by the method of Oseen approximation.

6) For oscillating flow [Eq. (30)], both the magnitude [0.5 in Eq. (30)] and the frequency [0.2 in Eq. (30)] have influence on the flow field. The important thing is the trajectory in the $x = \tau$ plane (Fig. 7). For instance, the trajectory of Eq. (30) lies between those of $a = 0$ and $a = 0.1$ of Eq. (29), the variation of Q_{max} with x for oscillating flow (30) also lies between those of $a = 0$ and $a = 0.1$.

7) All the results may be applied to the far-downstream wake too.

References

[1] Feldman, S., "On trails of axisymmetric hypersonic blunt bodies flying through the atmosphere," J. Aerospace Sci. **28**, 433–448 (1961).

[2] Pai, S. I., *Fluid Dynamics of Jets* (D. Van Nostrand Co., Inc., Princeton, N. J., 1954).

[3] Steiger, M. H. and Bloom, M. H., "Axially symmetric free mixing with swirl," Polytechnic Institute of Brooklyn Aeronautical Laboratory, PIBAL Rept. 628 (1960).

[4] Steiger, M. H. and Bloom, M. H., "Three dimensional viscous wakes," Polytechnic Institute of Brooklyn Aeronautical Laboratory, PIBAL Rept. 710 (1961).

[5] Zeiberg, S. L., "The wake behind an oscillating vehicle," J. Aerospace Sci. **29**, 1344–1346 (1962).